Neilands, J. B. (1977) *Adv. Chem. Ser. No. 162*, 3–32.
Ong, S. A., Peterson, T., & Neilands, J. B. (1979) *J. Biol. Chem. 254*, 1860–1865.
Pollack, J. R., & Neilands, J. B. (1970) *Biochem. Biophys. Res. Commun. 38*, 989–992.
Raymond, K. N., Isied, S. S., Brown, L. D., Fronczek, F. R., & Nibert, J. H. (1976) *J. Am. Chem. Soc. 98*, 1767–1774.
Ryler, A. P., Sanger, F., Smith, L. F., & Kitai, R. (1955) *Biochem. J. 60*, 541–556.
Sheldrick, G. (1976) *SHELX-76*, University Chemical Laboratory, Cambridge.
Suslow, T. V., Kloepper, J. W., Schroth, M. N., & Burr, T. J. (1979) *Calif. Agric. 33*, 15–17.
van der Helm, D., & Poling, M. (1976) *J. Am. Chem. Soc. 98*, 82–86.
van der Helm, D., Baker, J. R., Eng-Wilmot, D. L., Hossain, M. B., & Loghry, R. A. (1980) *J. Am. Chem. Soc. 102*, 4224–4231.

Structure of Pseudobactin A, a Second Siderophore from Plant Growth Promoting *Pseudomonas* B10†

Martin Teintze and John Leong*

ABSTRACT: The structure of nonfluorescent pseudobactin A, one of two extracellular siderophores (microbial iron transport agents) produced by the plant growth promoting bacterium *Pseudomonas* B10, was determined by comparison of its ^1H and ^{13}C NMR spectra with those of yellow-green, fluorescent pseudobactin, the other siderophore. The molecular and crystal structure of ferric pseudobactin is reported in the preceding paper in this issue [Teintze, M., Hossain, M. B., Barnes, C. L., Leong, J., & van der Helm, D. (1981) *Biochemistry* (preceding paper in this issue)]. The only structural difference between pseudobactin and pseudobactin A was that the latter was saturated at carbons 3 and 4 of the quinoline derivative, whereas pseudobactin is unsaturated at these positions. A mechanism is proposed for the observed conversion of pseudobactin A into pseudobactin in aqueous solution.

When cultured in iron-limiting, complex media, plant growth promoting *Pseudomonas* B10 produces the yellow-green, fluorescent siderophore (microbial iron transport agent) pseudobactin (Kloepper et al., 1980), whose molecular structure is described in the preceding paper in this issue (Teintze et al., 1981). We report here the isolation and structural characterization of yet another siderophore, pseudobactin A, from *Pseudomonas* B10. We also propose a rationale for the observed chemical conversion of pseudobactin A into pseudobactin.

Experimental Procedures

Siderophores. Ferric pseudobactin and pseudobactin were isolated from *Pseudomonas* B10 and purified as described previously (Teintze et al., 1981).

Ferric pseudobactin A and pseudobactin A were obtained from *Pseudomonas* B10 in an analogous fashion with the following modifications. *Pseudomonas* B10 was propagated in the aforementioned minimal medium except that the proteose peptone no. 3 was omitted. This medium is hereby referred to as the chemically defined, glycerol-based minimal medium. The cultures were harvested after 2–3 days. The CM-Sephadex C-25 column chromatography yielded a small red-brown band, which eluted ahead of a purple band consisting of ferric pseudobactin A, followed by a red-brown band containing ferric pseudobactin. The latter two bands overlapped. Ferric pseudobactin A was purified by Bio-Gel P-2 column chromatography as described in the preceding paper in this issue. The yield was typically 25–50 mg/Liter of culture supernatant fluids but varied considerably from run to run. The extinction coefficient of ferric pseudobactin A was obtained as described previously (Teintze et al., 1981).

Pseudobactin A was obtained by deferration of ferric pseudobactin A with 8-hydroxyquinoline according to an earlier procedure (Teintze et al., 1981). Fractions from the Bio-Gel P-2 column chromatography were assayed for iron-binding activity with $Fe(ClO_4)_3 \cdot xH_2O$ as described earlier except that the absorbance of the supernatant fluids at 533 nm was measured. The colorless, nonfluorescent, iron-binding band was concentrated to dryness in vacuo.

Pseudobactin and pseudobactin A were converted into their chloride salts by passing an aqueous solution through a short column containing DEAE-Sephadex A-25, chloride form, equilibrated in water. Both compounds were stored at −70 °C under high vacuum.

Chromatography. Thin-layer chromatography (TLC)[1] was performed as described in the preceding paper in this issue. Ferric pseudobactin A and pseudobactin A were homogeneous by TLC of their solutions.

Time Course of Production of Pseudobactin and Pseudobactin A. Siderophore production from *Pseudomonas* B10 was examined in detail in the chemically defined, glycerol-based minimal medium and in the same medium supplemented with 4 g of deferrated proteose peptone no. 3 per L. *Pseudomonas* B10 was propagated in King's medium B (KB) as described in the preceding paper in this issue. Approximately two drops each were transferred to 2.5 mL of minimal medium with and without proteose peptone no. 3, and these cultures were shaken

† From the Department of Chemistry, University of California at San Diego, La Jolla, California 92093. *Received March 24, 1981.* This work was supported in part by grants from the U.S. Public Health Service (AI 14084) and from the National Science Foundation (CHE-7916324) to the Southern California Regional NMR Facility.

[1] Abbreviations used: NMR, nuclear magnetic resonance; CD, circular dichroism; TLC, thin-layer chromatography; DSS, 3-(trimethylsilyl)propanesulfonic acid, sodium salt; Me_4Si, tetramethylsilane; Me_2SO, dimethyl sulfoxide; β-OH-Asp, β-hydroxyaspartic acid; KB, King's medium B; EDDA, ethylenediaminebis(*o*-hydroxyphenylacetic acid).

0006-2960/81/0420-6457$01.25/0

overnight at room temperature. Approximately 2 mL of each culture was transferred to 50 mL of the appropriate fresh medium, and the cultures were harvested by centrifugation shortly before they became yellow-green and fluorescent. The supplemented and unsupplemented cultures were harvested after approximately 12 and 36–48 h, respectively. After each cell pellet was washed 3 times with the appropriate fresh medium, it was suspended in a sufficient volume of the above-described medium to give an optical density of 0.5 at 650 nm. The cultures were shaken at room temperature, and 5-mL aliquots were removed at regular intervals and were centrifuged at 10000*g* for 5 min. After excess $Fe(NO_3)_3 \cdot 9H_2O$ was added to the supernatant fluids, the suspensions were saturated with ammonium sulfate. The resulting slurries were extracted with benzyl alcohol as described in the preceding paper in this issue. TLC was performed on the aqueous extracts from benzyl alcohol extractions as described above.

Reversal of Iron Starvation of Pseudomonas B10. The procedure of Ong et al. (1979) was followed. Briefly, molten KB agar containing 1.5% agar and 1 mg/mL ethylenediaminebis(*o*-hydroxyphenylacetic acid) (EDDA) was seeded with 1000 colony-forming units/mL of *Pseudomonas* B10 grown in KB medium. Filter paper disks containing 20 μL of the test solutions were placed on the surface of the solidified agar. Plates were incubated at room temperature and examined after 24, 30, and 36 h.

Spectroscopy. Proton NMR spectra were obtained at room temperature on a custom-designed 360-MHz spectrometer with 200–400 pulses in the Fourier-transform mode; carbon-13 NMR spectra were obtained at 5 °C by using 5000–8000 pulses in the Fourier-transform mode at 125.76 MHz on a Bruker WM 500 spectrometer located at the Southern California Regional NMR Facility, California Institute of Technology, Pasadena, CA. Visible spectra were measured with a Cary 17 spectrophotometer, and circular dichroism (CD) spectra were recorded on a Jasco J-10 spectropolarimeter.

Results

When cultured in iron-limiting, glycerol-based minimal medium, *Pseudomonas* B10 produced two iron-binding substances: the yellow-green, fluorescent siderophore pseudobactin and a colorless, nonfluorescent compound, which was assigned the trivial name pseudobactin A. Pseudobactin A exhibited properties typical of a siderophore, including complete repression of production in various culture media containing micromolar amounts of iron(III) (data not shown). Furthermore, pseudobactin and pseudobactin A and their ferric complexes, all at 10 μM, were about equally effective in reversing iron starvation of strain B10 induced by the synthetic ferric complexing agent EDDA, the iron of which is not utilized by the cells. This stimulation of growth was evidenced by a halo of single colonies surrounding the disks. In contrast, $FeCl_3$ at 10 mM was apparently required to saturate the EDDA in the medium, thereby producing similar-sized growth halos as the above compounds.

The visible and CD spectra of ferric pseudobactin and ferric pseudobactin A are shown in Figure 1. Red-brown ferric pseudobactin has an absorption maximum at 400 nm ($\epsilon = 2.0 \times 10^4$ L mol^{-1} cm^{-1}) with shoulders at 460 and 540 nm; yellow-green, fluorescent pseudobactin also has its absorption maximum at 400 nm ($\epsilon = 1.5 \times 10^4$ L mol^{-1} cm^{-1}) (Teintze et al., 1981). Purple ferric pseudobactin A had a broad absorption band with a maximum at 533 nm ($\epsilon = 2.5 \times 10^3$ L mol^{-1} cm^{-1}); its free ligand, nonfluorescent and colorless pseudobactin A, had no absorption maximum in the visible. Ferric pseudobactin has CD bands at 400 (2.0), 436 (−0.8),

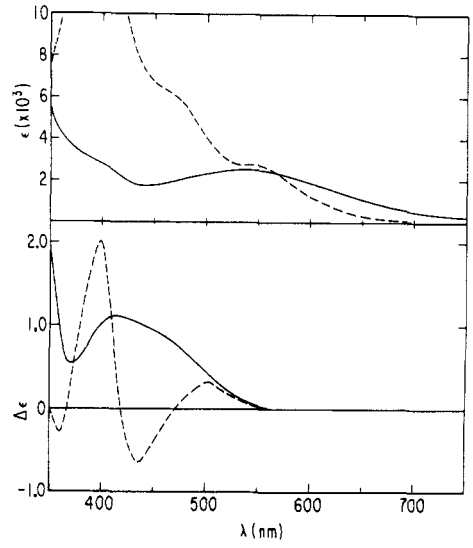

FIGURE 1: Visible and CD spectra of ferric pseudobactin A (—) and ferric pseudobactin (- - -) in aqueous solution.

and 502 (0.3) nm ($\Delta\epsilon$) (Teintze et al., 1981), whereas ferric pseudobactin A had only one CD band in the visible region at 410 (1.1) nm ($\Delta\epsilon$).

Aqueous solutions of pseudobactin A gradually turned yellow-green, fluorescent upon prolonged standing at room temperature at neutral pH. Both pseudobactin and pseudobactin A were detected in these solutions upon addition of iron(III), followed by isolation and characterization of ferric pseudobactin and ferric pseudobactin A by TLC. This conversion of pseudobactin A into pseudobactin was slow at neutral pH ($t_{1/2} \sim$ 2–3 days). The reaction was much faster in base ($t_{1/2} \sim$ 5 min at pH 10) but was not catalyzed by acid (pH 2). In the absence of oxygen, however, no conversion occurred even after 30 min at pH 10. Ferric pseudobactin A was stable indefinitely at room temperature and has not been observed to convert into ferric pseudobactin.

The production of pseudobactin and pseudobactin A by *Pseudomonas* B10 was monitored as a function of time in the glycerol-based minimal medium and in the same medium supplemented with proteose peptone no. 3 to determine whether pseudobactin was produced by strain B10 or simply arose from conversion of pseudobactin A. We previously demonstrated that only pseudobactin is isolated from a 48-h culture of strain B10 grown in the proteose peptone no. 3 medium (Kloepper et al., 1980). Pseudobactin and pseudobactin A were detected simultaneously as their ferric complexes in the glycerol medium, whereas only pseudobactin was detected in the proteose peptone no. 3 containing medium. Siderophore production typically commenced just before cells entered the stationary phase and continued even after cells reached the stationary phase. Thus, pseudobactin and pseudobactin A both appear to be natural products of *Pseudomonas* B10.

Amino acid analyses of pseudobactin A following hydrolysis in both 6 N HCl and 47% HI at 110 °C for 18 h showed the same amino acid composition as that of pseudobactin (Teintze et al., 1981). Since the basic conditions (pH 9, 37–40 °C) required for Edman degradations or dansyl amino-terminal analyses rapidly converted pseudobactin A into pseudobactin, no attempts were made to sequence the former.

The structure of pseudobactin A was determined from comparison of its ^1H and ^{13}C NMR spectra with those of pseudobactin, whose structure has been solved by X-ray diffraction (Teintze et al., 1981) and is shown in Figure 2. The

Table I: Proton NMR Chemical Shifts and Coupling Constants in D_2O

pseudobactin A			pseudobactin		
resonance	δ (ppm)	coupling constants (Hz)	resonance	δ (ppm)	coupling constants (Hz)
a	1.23	$J_{ap} = 6.4$	a	1.24	$J_{ap} = 6.4$
b	1.28		b	1.33	
c	1.42	$J_{cr} = 7.3$	c	1.43	$J_{cr} = 7.3$
	1.43			1.44	
d	1.49		d	1.57	
e	1.79	$J_{eo} = 6.5$	e	1.85	$J_{eo} = 6.4$
f	1.82		f	1.76	
	1.93			1.95	
g	2.00		g	2.00	
h	2.46		h	2.34	
i, j	2.64		i	2.73	$J_{ij} = 6.7$
			j	2.82	$J_{ji} = 6.7$
k	3.00	$J_{k_1v} = 11.9$ $J_{kk} = 16.0$			
	3.08	$J_{k_2v} = 6.2$			
l	3.24	$J_{ll} = 13$	l	3.28	$J_{ll} = 14$
	3.27			3.35	
m	3.44	$J_{mm} = 15, J_{mh} = 7.5$	m	3.39	$J_{mm} = 13$
	3.69			3.69	
n	3.61		n	3.59	$J_{nn} = 12$
	3.66			3.67	
o	4.05	$J_{oe} = 6.5$	o	4.10	$J_{oe} = 6.4$
p	4.12	$J_{pa} = 6.4, J_{pq} = 6.4$	p	4.14	$J_{pa} = 6.4, J_{pq} = 6.4$
q	4.32	$J_{qp} = 6.4$	q	4.33	$J_{qp} = 6.4$
r	4.36	$J_{rc} = 7.3$	r	4.37	$J_{rc} = 7.3$
	4.44			4.44	
s	4.47	$J_{sf_1} = 5.6, J_{sf_2} = 10.3$	s	4.48	$J_{sf_1} = 6.2, J_{sf_2} = 8.8$
t	4.56	$J_{tu} = 2.4$	t	4.55	$J_{tu} = 2.4$
u	4.92	$J_{ut} = 2.4$	u	4.91	$J_{ut} = 2.4$
v	5.05	$J_{vk_1} = 11.9, J_{vk_2} = 6.2$			
w	5.22		w	5.61	
x	6.86		x	7.04	
	6.90			7.15	
			y	7.91	

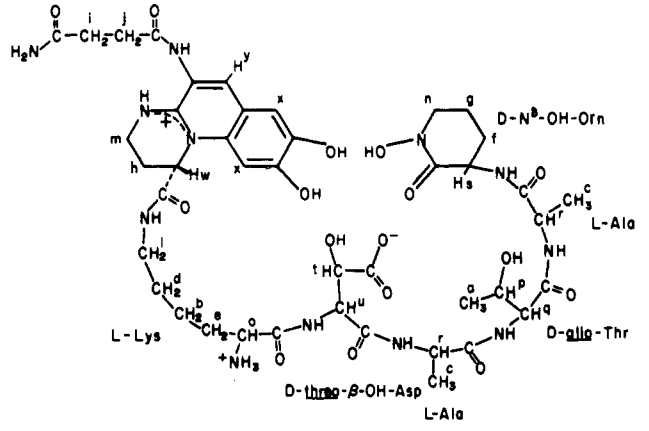

FIGURE 2: Structure of pseudobactin as determined from the crystal structure of ferric pseudobactin. The letters refer to the assignments in the ^1H NMR spectrum.

proton NMR spectra of pseudobactin A and pseudobactin in D_2O are shown in Figure 3; the resonances are also summarized in Table I. The letters assigned to the hydrogen atoms in Figure 2 refer to these ^1H NMR resonances. Assignments were made by comparison with previously reported chemical shifts of amino acid protons (Wüthrich, 1976), by comparison with spectra of partial sequences of pseudobactin (data not shown), and by irradiating each of the resonances in both spectra to determine which signals were coupled. Some of the chemical shifts and some of the geminal coupling constants listed in Table I were obtained from decoupling experiments (data not shown). The major differences between the two spectra in Figure 3 were the presence of a new singlet (y) at 7.91 ppm in pseudobactin and the absence of both the AB quartet (v) at 5.05 ppm and two superimposed AB quartets (k) centered at 3.00 and 3.08 ppm in pseudobactin. Resonances v and k in pseudobactin A were coupled to each other and integrated as one and two protons, respectively. The ^1H NMR spectra of pseudobactin A and pseudobactin in Me_2SO-d_6 from 6.5 to 10 ppm are shown in Figure 4. The resonances labeled x and y were assigned by titrating the samples with D_2O. All other resonances in this region disappeared upon addition of sufficient D_2O; the high-field regions of the Me_2SO-d_6 spectra were very similar to those of the respective compounds in D_2O, but the spectral resolution was not as good. The amide doublet at 8.81 ppm in the Me_2SO-d_6 spectrum of pseudobactin A was coupled to proton v, which was a multiplet at 4.91 ppm. The amide doublet at 8.47 ppm in the same spectrum was coupled to proton u at 4.72 ppm, which was therefore assigned as the C^{α}-H of the *threo*-β-hydroxyaspartic acid residue; the amide doublet at 7.96 ppm was coupled to the C^{α}-H resonance of *allo*-Thr at 4.17 ppm. The amide doublets at 8.10, 8.03, and 7.98 ppm in the pseudobactin A spectrum were coupled to the three C^{α}-H resonances between 4.25 and 4.35 ppm, but the latter were not resolved sufficiently in Me_2SO-d_6 to permit their identification. The corresponding C^{α}-H resonances in the pseudobactin spectrum were also not resolved, and some of the amide protons were obscured by the aromatic proton resonance (y) at 7.96 ppm. Only the amide resonance at 8.66 ppm could be assigned as that of β-OH-Asp. The singlets at 7.64 and 7.07 ppm in the Me_2SO-d_6 spectrum of pseudobactin A and the singlets at 7.57 and 7.00 ppm in that of pseudobactin were probably due to the hydroxyl protons of β-OH-Asp and *allo*-Thr but could not be assigned unequivocally.

The proton-decoupled ^{13}C NMR spectra of pseudobactin A and pseudobactin in D_2O are shown in Figure 5. The spectrum of pseudobactin was consistent with the structure

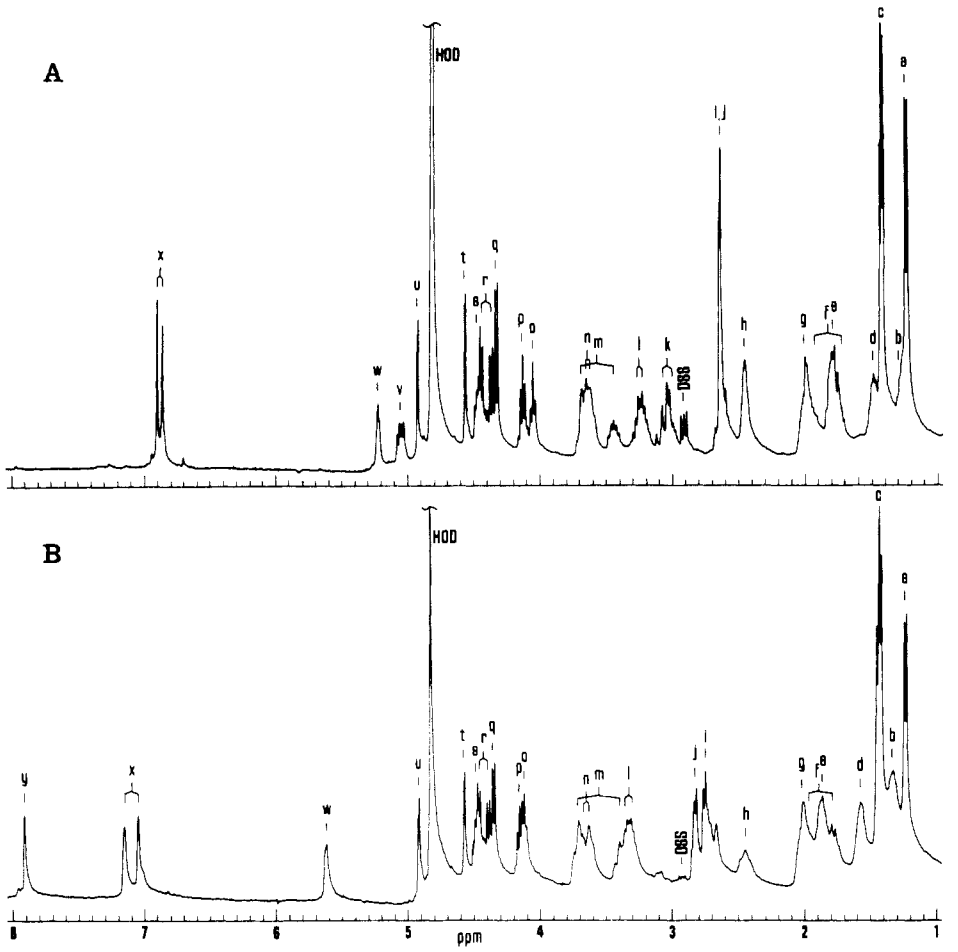

FIGURE 3: ^1H NMR spectra (360 MHz) of pseudobactin A (A) and pseudobactin (B) in D_2O. Chemical shifts are in parts per million from internal DSS.

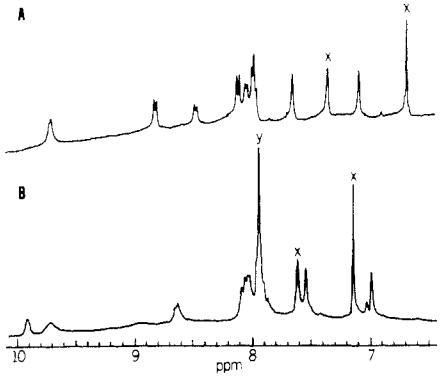

FIGURE 4: ^1H NMR spectra (360 MHz) of pseudobactin A (A) and pseudobactin (B) in Me_2SO-d_6. Chemical shifts are in parts per million from internal Me_4Si. Only the region from 6.5 to 10.0 ppm is shown.

shown in Figure 2; ten carbonyl carbon resonances occurred between 167 and 178 ppm, nine aromatic carbon resonances between 101 and 152 ppm, and 23 aliphatic carbon resonances between 17 and 73 ppm from Me_4Si. The peaks at 171.97 and 172.01 ppm, those at 50.53, 50.80, and 50.88 ppm, those at 31.09 and 31.27 ppm, and those at 17.07 and 17.29 ppm might be too close together to be distinguishable in the figure. Three of the aromatic carbon resonances (at 139.6, 114.5, and 101.0 ppm) were split into doublets in an undecoupled ^{13}C NMR spectrum (data not shown); thus, these three aromatic carbons each had a hydrogen atom attached, as expected from the structure and confirmed in the ^1H NMR spectrum (Figure 3). The ten carbonyl carbon resonances of pseudobactin A had chemical shifts nearly identical with those in pseudobactin (Figure 5). The peaks at 171.93 and 172.02 ppm might be difficult to distinguish in the figure. Two fewer resonances, however, occurred in the aromatic carbon region of pseudobactin A, and one of these was quite far downfield at 160.7 ppm. The resonances at 116.8 and 105.4 ppm split into doublets in an undecoupled ^{13}C NMR spectrum (data not shown), indicating that these carbons each were attached to a hydrogen atom. Pseudobactin A had additional resonances at 47.9 and 28.6 ppm in the ^1H-decoupled ^{13}C NMR spectrum where none occurred in pseudobactin (Figure 5); these two resonances were a doublet and a triplet, respectively, in the undecoupled spectrum (data not shown). Thus, these two carbons were bonded to one hydrogen and two hydrogens, respectively. The remaining resonances of pseudobactin A in the aliphatic region had chemical shifts nearly identical with those of pseudobactin (Figure 5). Pseudobactin had resonances at 50.80 and 50.88 ppm, however, pseudobactin A had only one at 50.83 ppm; pseudobactin also had resonances at 31.27 and 31.09 ppm, whereas pseudobactin A had only one at 31.17 ppm. These differences must have been due to these resonances not resolving in the pseudobactin A spectrum because the ^1H NMR data were not consistent with pseudobactin A having two carbon atoms less than pseudobactin (vide infra).

The above data indicated that pseudobactin A had the structure shown in Figure 6, which differed from that of pseudobactin only in that the bond between atoms 3 and 4 of the quinoline ring system was saturated in pseudobactin A. Thus, the observed conversion of pseudobactin A into pseudobactin was an oxidation of this bond, resulting in the loss of two hydrogen atoms and the formation of a second aromatic ring. This increase in conjugation explains the appearance

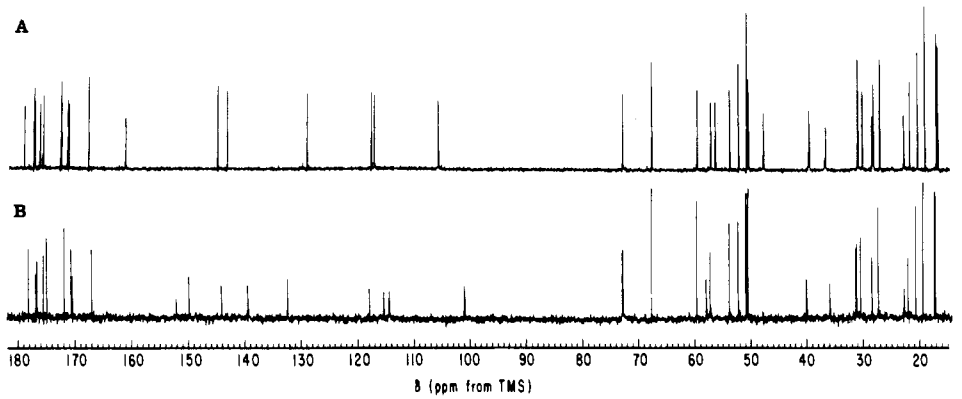

FIGURE 5: ^1H broad-band-decoupled ^{13}C NMR spectra of pseudobactin A (A) and pseudobactin (B) at 125.76 MHz in D_2O. Chemical shifts are relative to Me_4Si.

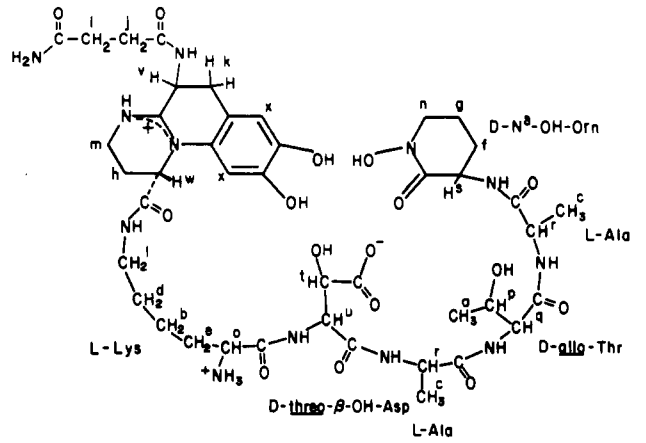

FIGURE 6: Proposed structure of pseudobactin A. The letters refer to the assignments in the ^1H NMR spectrum.

of the visible absorption band and the fluorescence in pseudobactin and agrees with the ^{13}C NMR data which showed two additional aromatic carbons in pseudobactin, one of which had a hydrogen attached. The carbon atom with the partial positive charge between the two nitrogen atoms absorbed at 160.7 ppm in the pseudobactin A spectrum but moved at least 8.5 ppm upfield in pseudobactin as a result of this increase in conjugation and the fact that resonance structures with the positive charge on the nitrogen atoms were more favored in the pseudobactin structure. The ^{13}C chemical shifts of the new peaks in the pseudobactin A spectrum at 47.9 and 28.6 ppm agreed with values reported for carbons adjacent to amide nitrogens and aromatic rings, respectively (Sadtler Research Laboratories, 1980a). The undecoupled spectrum showed that these carbons had the correct number of attached hydrogens, as predicted from the structure in Figure 6. These hydrogen atoms gave rise to resonances v and k in the ^1H NMR spectrum of pseudobactin A (Figure 3); these chemical shifts were consistent with those of protons in these two environments (Pouchert & Campbell, 1974; Sadtler Research Laboratories, 1980b). The coupling of resonance v to the protons at k and an amide proton confirmed this assignment. The carbon at which proton v and the succinyl diamide moiety were attached was an asymmetric center. This caused the protons designated k to be nonequivalent and resulted in the splitting patterns observed for resonances v and k. When pseudobactin A converted to pseudobactin, these two resonances disappeared, and a new aromatic proton singlet (y) appeared at 7.91 ppm as expected from the structure in Figure 2. The structures shown in Figures 2 and 6 also accounted for the minor differences between the two ^1H NMR spectra shown in Figure 3. The fact that the resonance of protons j moved downfield from that of protons i in the pseudobactin spectrum could have been due to the former being closer to the newly created aromatic ring. The proton labeled w, which was also close to this aromatic ring as well as to a more positive nitrogen in pseudobactin, also moved downfield. All of the resonances of the lysine residue also moved slightly downfield in the pseudobactin spectrum (Figure 3), but all the signals from the remainder of the peptide chain were identical in both compounds.

Discussion

The chemical and structural evidence presented above suggests the following mechanism for conversion of pseudobactin A into pseudobactin:

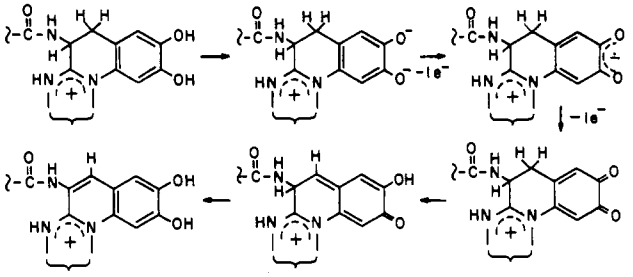

The first step, dissociation to the catecholate dianion, would be facilitated by the electron-withdrawing effect of the positively charged nitrogen para to one of the hydroxyl groups. The pK_as of the two hydroxyls might not be as low as those of 4-nitrocatechol, which has pK_as of 6.65 and 10.80 compared to 9.22 and 13.00 for catechol (Avdeef et al., 1978), but even at neutral pH, enough of the catecholate dianion might be present for the reaction to proceed at the slow rate observed. The air oxidation of catecholate dianion to *o*-benzoquinone is well-known and proceeds in sequential one-electron steps via *o*-benzosemiquinone. The mechanism shown above would account for the greatly increased rate of oxidation in base and the lack of conversion in the absence of oxygen. The driving force for the base-catalyzed air oxidation would be the formation of a second aromatic ring. A mechanism of this type has been observed for the air oxidation of 2,3-dihydro-5,6-dihydroxyindole-2-carboxylic acid and its methyl ester to 5,6-dihydroxyindole-2-carboxylic acid and the corresponding methyl ester. These air oxidations are also slow in neutral solution and rapid in base and can be prevented by excluding oxygen (Wyler & Dreiding, 1962). The iron(III) in ferric pseudobactin A prevented the oxidation of the catecholate dianion, presumably by acting as a Lewis acid. An alternative mechanism involving a monoanion was judged unlikely, be-

cause the preferred monoanion has the 6-hydroxyl proton of the quinoline derivative ionized and would not lead to the desired product.

Although pseudobactin A converted spontaneously into pseudobactin in aqueous solution, both compounds were natural products of *Pseudomonas* B10. Pseudobactin A was produced only in iron-limiting, chemically defined minimal media, whereas pseudobactin production occurred even in nutritionally richer iron-deficient media. Pseudobactin A, but not ferric pseudobactin A, exhibited in vitro antibiosis against the bacterium *Erwinia carotovora*, which causes potato soft rot and seedpiece decay (data not shown). Analogous results have been reported for pseudobactin and ferric pseudobactin (Kloepper et al., 1980). The ability of pseudobactin A to promote plant growth or control phytopathogenic microorganisms in soils cannot be distinguished from that of pseudobactin, because pseudobactin A converts into the latter during the time course of the experiments.

Both ferric pseudobactin and ferric pseudobactin A are equally efficient at transporting iron into *Pseudomonas* B10 (J. Leong, unpublished experiments). The reason why *Pseudomonas* B10 should produce two siderophores is not evident nor are the biological implications of the chemical conversion immediately obvious.

The absolute configuration about the iron in ferric pseudobactin A could not be determined from its relatively featureless visible CD spectrum. The configuration of the additional chiral carbon in pseudobactin A is also not known. The determination of the X-ray structure of ferric pseudobactin A, which is now in progress (D. van der Helm, unpublished experiments), could answer these questions.

Acknowledgments

We thank Drs. H. A. Itano and R. F. Doolittle for the use of their equipment and Dr. J. M. Wright and the staff of the Southern California Regional NMR Facility for technical assistance.

References

Avdeef, A., Sofen, S. R., Bregante, T. L., & Raymond, K. N. (1978) *J. Am. Chem. Soc. 100*, 5362-5370.

Kloepper, J. W., Leong, J., Teintze, M., & Schroth, M. N. (1980) *Nature (London) 286*, 885-886.

Ong, S. A., Peterson, T., & Neilands, J. B. (1979) *J. Biol. Chem. 254*, 1860-1865.

Pouchert, C. J., & Campbell, J. R. (1974) *The Aldrich Library of NMR Spectra*, Aldrich Chemical Co., Inc., Milwaukee, WI.

Sadtler Research Laboratories (1980a) *Sadtler Standard Carbon-13 NMR Spectra*, Philadelphia, PA.

Sadtler Research Laboratories (1980b) *Sadtler Standard Proton NMR Collection*, Philadelphia, PA.

Teintze, M., Hossain, M. B., Barnes, C. L., Leong, J., & van der Helm, D. (1981) *Biochemistry* (preceding paper in this issue).

Wüthrich, K. (1976) *NMR in Biological Research: Peptides and Proteins*, pp 42-55, North-Holland/American Elsevier, New York.

Wyler, H., & Dreiding, A. S. (1962) *Helv. Chim. Acta 45*, 638-640.

Direct Determination of the Protonation States of Aspartic Acid-102 and Histidine-57 in the Tetrahedral Intermediate of the Serine Proteases: Neutron Structure of Trypsin†

Anthony A. Kossiakoff* and Steven A. Spencer‡

ABSTRACT: A neutron structure analysis at 2.2-Å resolution has been performed on bovine trypsin covalently inhibited by a transition-state analogue, the monoisopropylphosphoryl (MIP) group. The unique ability of neutron diffraction to locate hydrogen atoms experimentally has allowed the determination of the protonation states of the catalytic site residues (Asp-102 and His-57). Since the bound MIP group mimics the tetrahedral intermediate structure, these correspond to the protonation states at the most crucial step of the hydrolysis. This has resolved a much debated mechanistic issue by showing conclusively that the catalytic base in the transition state of the reaction is His-57, not Asp-102. This finding has important implications for the understanding of the hydrolysis mechanism of the serine proteases. A detailed examination of the stereochemical interaction among the catalytic groups was also conducted to identify their individual roles in the mechanism. Besides functioning as the catalytic group, it was found that His-57 could effectively "steer" the attacking water toward the acyl group during deacylation. Other aspects of protein structure which are observable only by neutron diffraction analysis are also discussed. These include orientation of well-ordered amide side chains, which is made possible by the large scattering difference between nitrogen and oxygen atoms, location and orientation of water molecules, and hydrogen exchange properties of the protein.

A major shortcoming of X-ray determinations of protein structures is that the locations of the hydrogen atoms cannot be observed directly and therefore must be inferred from the stereochemistry of the heavier atoms. This method of extrapolating hydrogen positions makes it difficult to define accurately the chemical interactions taking place among groups within the protein, especially since any unusual or unexpected stereochemistry for the hydrogens will be overlooked. Since a large number of the total atoms in a protein are hydrogen, and since much of the chemistry of proteins involves hydrogen

† From the Biology Department, Brookhaven National Laboratory, Upton, New York 11973. *Received February 12, 1981; revised manuscript received June 30, 1981.* Research carried out at Brookhaven National Laboratory was under the auspices of the U.S. Department of Energy.

‡ Present address: Genentech Inc., South San Francisco, CA 94080.

0006-2960/81/0420-6462$01.25/0